ENERGY AND EXERGY ANALYSIS OF HYBRID REFRIGERATION SYSTEMS

By

Karanjit Singh	**21117058**
Nikita	**21117082**
Varnit Gupta	**21117140**

DEPARTMENT OF MECHANICAL AND INDUSTRIAL ENGINEERING

INDIAN INSTITUTE OF TECHNOLOGY ROORKEE

2024-25

CERTIFICATE

This is to certify that the thesis entitled "**Energy and Exergy Analysis of Hybrid Refrigeration Systems"** being submitted by **Karanjit Singh, Nikita and Varnit Gupta** to the Department of Mechanical and Industrial Engineering, **Indian Institute of Technology Roorkee (India)** for the fulfillment of the curriculum requirements to obtain the degree of **Bachelor of Technology** is a bona fide work carried out by them under my guidance and supervision. The content of this thesis, in full or in part, has not been submitted elsewhere for the award of any other degree or diploma.

Nikhil Kumar Singh
Assistant Professor
Department of Mechanical and Industrial Engineering
Indian Institute of Technology Roorkee
Uttarakhand – 247667, INDIA

SELF DECLARATION AND ACKNOWLEDGEMENTS

We hereby declare that the work carried out in this report entitled, "***Energy and Exergy Analysis of Hybrid Refrigeration Systems***", is presented for the course MIN-400A/B: B.Tech Project submitted to the Department of Mechanical and Industrial Engineering, Indian Institute of Technology Roorkee (India), is an authentic record of our own work carried out under the supervision of Prof. Nikhil Kumar Singh, MIED, IIT Roorkee. We have not submitted the record embodied in this project report for the award of any other degree or diploma in any institute.

We thank Professor Nikhil Kumar Singh, esteemed faculty of the department of Mechanical and Industrial Engineering at IIT Roorkee for his guidance and support throughout our final year B. Tech project. Professor Nikhil Kumar Singh's profound expertise and mentorship have played a pivotal role in shaping our research endeavours. We sincerely appreciate his encouragement and feedback, which have greatly enriched the quality of our work. We remain deeply indebted to him for his invaluable mentorship and unwavering support. This project helped us in understanding the practical application of refrigeration systems and allowed us to experiment with different configurations.

Karanjit Singh **21117058**

Nikita **21117082**

Varnit Gupta **21117140**

ABSTRACT

This project aims to analyse various configurations of a combined refrigeration cycle designed to enhance energy efficiency by evaluating the thermodynamic performance of a system that couples two refrigeration cycles. Our approach involves combining a refrigeration system that releases heat(as waste) at a high and combining it with a system that uses low grade heat hence utilising waste heat.

A simulation program is developed using python to evaluate COP and exergetic efficiency of TCRS combined with single effect, series flow double effect and parallel flow double effect systems over a range of evaporator temperature and gas cooler pressure, followed by a comparison of the same.

The comparative analysis shows that at constant generator pressure, the combined parallel flow VARS system outperforms the series flow system in terms of COP and exergetic efficiency when the distribution ratio (D) is below 0.57. The parallel system achieves a 18.06% higher COP than TCRS and 1.86% higher than the series system, with exergetic efficiency improving by 4.66% over TCRS and 0.53% over the series configuration.

TABLE OF CONTENTS

LIST OF FIGURES

LIST OF TABLES

NOMENCLATURE

T	*Temperature (in degree C)*
P	*Pressure (in MPa)*
H	*Specific enthalpy(kJ/kg)*
S	*Specific entropy(kJ/kg.K)*
D	*Distribution ratio*
gc	*Gas cooler*
x	*Mass fraction of Lithium Bromide*
$\dot{Q}$	*Heat flow rate*
η_t	*Efficiency of turbine*
η_c	*Efficiency of compressor*

Abbreviations

TCRS	*Transcritical refrigeration system*
VARS	*Vapour absorption refrigeration system*
VCRS	*Vapour compression refrigeration system*
HPG	*High pressure generator*
LPG	*Low pressure generator*
SHX	*Solution heat exchangers*
COP	*Coefficient of performance*
a	*Absorber*
cond	*Condenser*
c	*Compressor*
g	*Generator*

CHAPTER 1: INTRODUCTION

1.1 Background

a. Refrigeration System

A refrigeration system is a system of thermodynamic processes that removes heat from a space or substance to lower and maintain its temperature below the surrounding environment. It operates on the principles of thermodynamics and typically involves a working fluid (refrigerant) that undergoes phase changes to absorb and reject heat.

b. Types of Refrigeration Systems

Vapor Compression Refrigeration System (VCRS): VCRS is the most common refrigeration system, using a refrigerant to transfer heat through compression and expansion. It consists of four key components: compressor, condenser, expansion valve, and evaporator. Refrigerant pressure is increased with help of compressor, the condenser releases heat, the expansion valve reduces pressure, and the evaporator absorbs heat for cooling.

Vapor Absorption Refrigeration System (VARS): This system uses a heat-driven absorption process instead of a mechanical compressor. It typically involves a refrigerant-absorbent pair, such as ammonia-water or lithium bromide-water, making it suitable for uses where waste heat or solar energy is available. The basic VARS setup comprises key components: absorber, pump, generator, solution heat exchanger, condenser, expansion device, and evaporator. The absorber, pump, solution heat exchanger, expansion valve, and generator replace the compressor.

Transcritical Refrigeration System (TCRS): This system operates above the critical pressure of the refrigerant, typically CO_2, which does not condense in the high-pressure side but rather undergoes cooling and expansion. In these systems, CO2 can exist in a supercritical state, where it behaves like a gas and a liquid simultaneously, and a subcritical state, where it acts like a conventional refrigerant. TCRS includes a compressor, a gas cooler, an expansion valve, and an evaporator.

c. Hybrid Refrigeration System

A hybrid system combines different refrigeration systems, VARS and TCRS in this case, to enhance efficiency, reduce energy use, and utilize waste heat.

d. Types of VARS

Single Effect VARS: A single-effect Vapor Absorption Refrigeration System operates using a basic absorption cycle that includes an absorber, generator, evaporator, and condenser connected in a loop. In this system, vapor from the evaporator flows into the absorber, where it gets absorbed by the weak solution while the absorption heat is removed.

Double Effect VARS: A double-effect Vapour Absorption Refrigeration System is an advanced cooling system that uses two generators, allowing regeneration in two stages, which results in a higher Coefficient of Performance (COP) and efficiency compared to a single-effect system.

e. Configurations of Double Effect VARS:

There are two configurations of Double Effect VARS:

Series flow double effect absorption refrigeration system: The series flow consists of two generators (LPG and HPG), evaporator, condenser, absorber, pump, two solution heat exchanger, and expansion valves. The solution is pumped to the heat exchangers from the absorber and then to the HPG where the solution is then heated such that it boils out the refrigerant vapour from the solution. The vapour from HPG then comes into the LPG, thus heating the solution and being condensed. The heat of condensation of primary vapour obtained from HPG is utilised in LPG to further obtain secondary vapour.

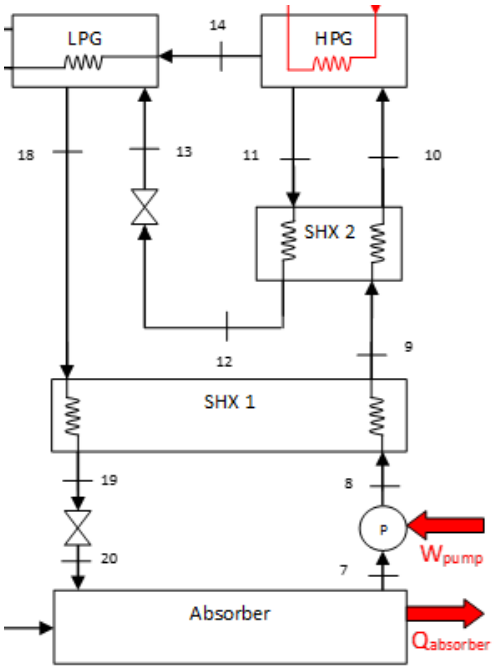

Figure 1.1: Diagram of series flow double effect absorption refrigeration system.

Parallel flow double effect absorption refrigeration system: As mentioned above the refrigeration cycle mainly consists of two generators, i.e. HPG (high-pressure generator), and LPG (low-pressure generator), other than that it also contains two solution heat exchangers, absorber, evaporator, expansion valves, condenser, and solution pump. The process involves the solution traveling from the absorber and then it is pumped and then it is directed to the two parallel free streams to the HPG and the LPG, respectively.

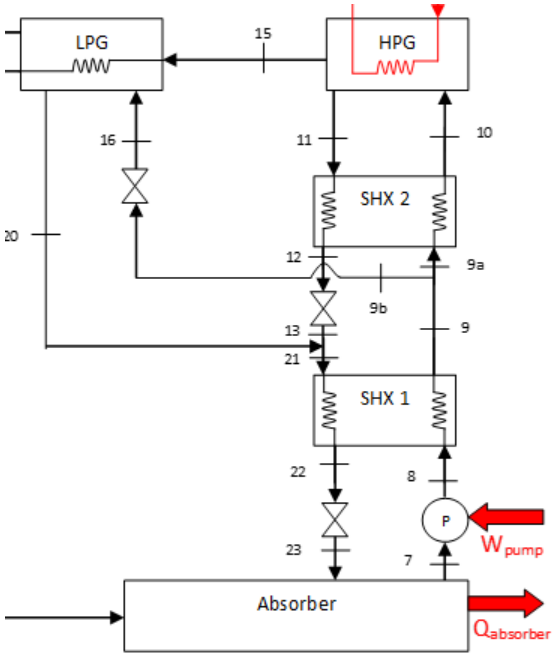

Figure 1.2: Schematic of parallel flow double effect absorption refrigeration system.

In this study it is proposed to use a hybrid system such that, TCRS works as the primary refrigeration system, which provides primary cooling, and VARS uses the low-grade energy rejected by TCRS working as a secondary refrigeration system.

f. Why TCRS and not VCRS?

Traditional Vapor Compression Refrigeration Systems (VCRS) rely on condensation at a lower temperature to convert the refrigerant from a gas to a liquid. However, CO_2 has a very low critical temperature of 31.1°C, meaning that in warm climates or high-temperature conditions, it becomes difficult to condense CO_2 efficiently. To achieve condensation in such conditions, the system would require extremely high pressures, making it impractical and inefficient. As a result, CO_2-based VCRS struggles to operate effectively in environments where ambient temperatures exceed 31°C. In contrast, a Transcritical Refrigeration System (TCRS) does not rely on condensation but instead uses a gas cooler to reject heat, making it more suitable for CO_2 refrigeration. This ability to operate efficiently at high pressures and temperatures makes TCRS the preferred choice for CO_2 as a refrigerant.

1.2 Motivation

In a conventional refrigeration system, the heat that is rejected is considered as a loss for the system, costing us efficiency. However, this waste heat can be effectively utilized to enhance the overall system performance, which is where hybrid refrigeration systems play a crucial role. A hybrid system uses the rejected heat from one cycle to drive another cycle, which leads to improved efficiency and Coefficient of Performance (COP). This not only allows for better energy management and increase in efficiency but also makes the system more sustainable.

During our project we also considered selection of environmentally friendly refrigerants for refrigeration systems to minimize the impact on global warming and ozone depletion. Traditional refrigerants often contribute to greenhouse gas emissions, making the shift to eco-friendly alternatives is also essential.

Natural refrigerants like air, water vapor, hydrocarbons, ammonia, and carbon dioxide offer sustainable alternatives for cooling applications. Among these, CO_2 has gained widespread adoption due to its versatility in residential, commercial, and industrial refrigeration, as well as in air conditioning systems. It is a safe choice due to its non-toxic and non-flammable properties, along with being cost-effective and readily available. Since CO_2 is a byproduct of industrial processes, its overall contribution to global warming is neutral, despite having a Global Warming Potential (GWP) of 1.

To evaluate the effectiveness of hybrid refrigeration systems we implemented the first and second laws of thermodynamics fundamental insights. We aimed to evaluate the Coefficient of Performance (COP) which measures the system's efficiency in converting input energy into cooling, and exergetic efficiency which helped us assess how effectively available energy is utilized. By analysing these parameters, we designed hybrid refrigeration systems that had an increased COP and exergetic efficiency, reduced waste heat losses, and contributed to sustainable thermal management solutions.

1.3 Applications

Hybrid refrigeration systems have diverse applications across various industries, offering improved energy efficiency and sustainability. Hybrid refrigeration systems are used in food processing, cold storage, and pharmaceutical sectors.

In this case, we have designed our hybrid system with the presence of two evaporators (which means we have two different refrigeration systems) such that the range of the evaporator in TCRS is -35 °C to -15 °C and in VARS nearby 7 °C.

One of the major applications, in the above range of parameters are hybrid refrigeration systems used in ice cream factories, where blast chillers operate around -27 °C and ingredients are stored around 6 °C.

CHAPTER 2: LITERATURE REVIEW

The growing demand for energy-efficient and sustainable refrigeration systems has driven significant research into advanced thermodynamic cycles, particularly those leveraging waste heat recovery and multi-effect absorption technologies.

Haq et al. (2022) introduced an optimized self-condensing transcritical CO_2 cycle for hot climates, achieving a thermal efficiency of 39.82% and an exergy efficiency of 67.65%. The design incorporates dual recuperators to minimize irreversibility and avoids near-critical operations, simplifying turbomachinery requirements. Dubey et al. (2014) proposed a transcritical cascade system using propylene (R1270) in the low-temperature cycle and CO_2 in the high-temperature cycle. This configuration demonstrated superior thermal performance compared to subcritical and N_2O–CO_2 systems, with optimized parameters and design guidelines developed for practical applications. Vaccaro et al. (2023) investigated the performance improvement of CO_2 transcritical refrigeration cycles by adding secondary components. Their study identified R1234yf as the most effective additive due to its flat evaporation curve, which optimizes heat exchange. Mixtures containing up to 15% R1234yf enhanced the coefficient of performance (COP) across multiple cycle configurations compared to pure CO_2.

Ma and Deng (1996) conducted a theoretical analysis of a two-stage LiBr/H_2O absorption refrigeration system driven by low-temperature heat sources (75–87°C), demonstrating its viability for waste heat recovery and solar energy applications. The analysis revealed that COP improves with increasing heat source temperature but plateaus beyond 87°C, while performance declines sharply if chilled water temperatures fall below 7°C or cooling water temperatures exceed 32°C. Gomri (2009) performed a second-law comparison of single- and double-effect LiBr/H_2O absorption refrigeration systems. The study revealed that while the double-effect system achieves a significantly higher COP (1.22–1.42) compared to the single-effect system (0.73–0.79), its exergetic efficiency improvement is modest (14.3–25.1% vs. 12.5–23.2%). Optimal generator temperatures were identified (70–90°C for single-effect, 130–150°C for double-effect) to minimize exergy destruction and maximize both COP and exergy efficiency. Kaita (2002) evaluated three triple-effect LiBr-H_2O absorption cycles (parallel-flow, series-flow, and reverse-flow), revealing that the parallel-flow configuration achieves the highest COP (~1.83–2.17). The reverse-flow cycle exhibits lower maximum pressures (<300 kPa) and temperatures, enhancing material durability. Sensitivity analysis highlighted that COP is most influenced by solution heat exchangers, whereas maximum pressure and temperature depend on medium-temperature generator (MTG) and low-temperature generator (LTG) performance. The reverse-flow cycle balances efficiency (COP ~1.8) with operational safety (pressure ~300 kPa, reduced corrosion risk). Xu et al. (1996) analyzed a double-effect series-flow absorption chiller using H_2O/LiBr, focusing on design parameters like heat recovery ratios and solution circulation ratio (a). Results showed

that increasing heat recovery ratios and reducing the circulation ratio (a = 12) improved the COP to 1.227, while minimizing the total heat transfer area to 100 m^2 for a 350 kW system. Although exergy efficiency was not explicitly calculated, the optimization balanced performance (COP) and cost (heat transfer area).

Arora et al. (2011) analyzed a combined transcritical CO_2 compression refrigeration system (TCRS) and single-effect H_2O-LiBr absorption system (VARS), utilizing waste heat from the TCRS gas cooler to enhance efficiency. At an evaporator temperature of −25°C, the combined system achieved a 14.2% increase in COP (from 1.69 to 1.93) and a 3.67% rise in exergetic efficiency (from 30% to 31.1%) compared to standalone TCRS. The system's performance is most pronounced at lower evaporator temperatures, with refrigerating capacity improvements up to 49.8%. Siddique et al. (2025) proposed four novel systems combining double-effect absorption refrigeration cycles with vapor compression refrigeration systems (VCRS). Their results showed that the double-effect absorption cycle offered significant improvements in COP and exergy performance over traditional configurations. The study further highlighted the impact of operational parameters such as evaporator temperature, entrainment ratio, and ejector pressure drop on system performance. These findings suggest a promising strategy for efficient low-temperature cooling with better waste heat utilization. Yang et al. (2021) presented an innovative approach to low-grade waste heat recovery by combining absorption refrigeration with a transcritical CO_2 power cycle. Through a detailed 3E analysis—encompassing energy, economic, and environmental factors—the multi-objective optimization highlighted a balance between energy efficiency and environmental performance, demonstrating a 13.17% improvement in thermal efficiency and a 13.49% reduction in environmental impact, with a manageable increase in costs. This research underscores the potential for integrating energy systems to achieve both economic and environmental benefits.

Recent studies have demonstrated the potential of transcritical CO_2 (TCRS) and absorption refrigeration systems (VARS) individually. However, limited work has systematically compared integrated configurations—especially TCRS combined with single- and double-effect LiBr/H_2O VARS consisting of two evaporators for two separate applications and operating at different temperature ranges. In our project, we will examine TCRS combined with three different systems: single-effect VARS, series-flow double-effect VARS, and parallel-flow double-effect VARS. We will compare their COP and exergetic performances over various parameters such as gas cooler pressure and evaporator temperature.

CHAPTER 3: METHODOLOGY

The present research commenced with a thorough review of conventional and advanced refrigeration systems to evaluate their thermodynamic performance and suitability for specific applications. This foundational study enabled us to identify promising configurations and subsequently conceptualize two hybrid refrigeration systems—one utilizing a series flow configuration and the other a parallel flow configuration—designed for a dual-evaporator application with distinct temperature ranges.

We applied mass, energy, and exergy balances to analyze both systems, focusing on the H_2O/LiBr pair and accounting for phase change and concentration effects using literature-based property correlations. The computational framework was developed in Python, where a detailed set of over 200 thermodynamic equations was implemented for each configuration. The CoolProp library was employed to retrieve accurate refrigerant properties, while SymPy handled the symbolic manipulation and solution of nonlinear algebraic equations. Additional numerical operations were executed using NumPy. This integrated simulation environment enabled iterative performance evaluations across various design parameters.

To validate the model, we replicated results from Arora et al. (2011), which confirmed the accuracy of our framework. Simulation results showed that the parallel configuration outperformed the series one, particularly at lower distribution ratios, in terms of COP and exergetic efficiency.

3.1 System Description

a. Combined TCRS - single effect VARS:

The system has a TCRS combined with a single effect VARS as shown in Figure 3.1.

In TCRS the refrigerant, carbon dioxide (CO_2), enters the evaporator, where it absorbs heat from the refrigerated space and changes into saturated vapor state and further, it is compressed to point 2. The waste heat from gas cooler 1 is then supplied to a different stream which will give the heat to the generator of VARS. Then the heat is released is in gas cooler 2 and the refrigerant further cools down. Finally, the refrigerant expands in a turbine, which generates power. The turbine is connected with the compressor, and the power produced helps drive the compressor. The same process is shown in Figure 3.2 where 1—2 is compression, 2—3 is cooling in gas cooler 1, 3—4 is cooling in gas cooler 2, 4—5 is expansion process and 5—1 is evaporation process (refrigeration effect).

In the Single-Effect Vapor Absorption Refrigeration System (VARS), a solution of LiBr and water is used as the working pair, where H_2O acts as the refrigerant and LiBr solution as absorbent. The process begins in the evaporator, where liquid water preforms refrigeration effect by absorbing heat from the refrigerated space and

evaporates. The water vapor then enters the absorber, where it is absorbed by the LiBr solution, forming a strong solution. This absorption process releases heat. The strong solution is then pumped to the generator, where it is heated using an external heat source—typically steam, hot water, or waste heat. In this case, the generator is supplied, which is rejected by the primary TCRS gas cooler 1. This heat causes the refrigerant to separate from the LiBr solution as vapor. The remaining weak solution is returned to the absorber for recirculation. The water vapor from the generator then condensed within the condenser and cools down by releasing the heat to either an air-cooled type condenser or a water-cooled type condenser. The condensed water passes through an expansion valve, where its pressure is reduced before entering the evaporator, completing the cycle. The P-T-X graph of the states are shown in Figure 3.3. 7—9 is compression by pump, then separation of water vapour from solution(9—14), expansion is shown by 14—6 and 10—12.

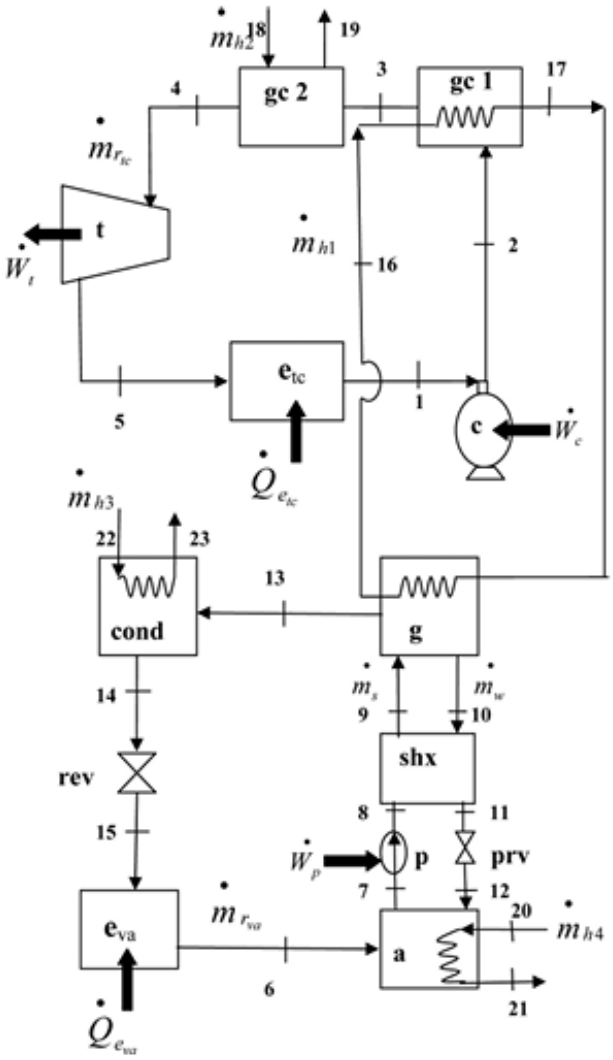

Figure 3.1: Schematic of a TCRS integrated with a single effect VARS **[15]**.

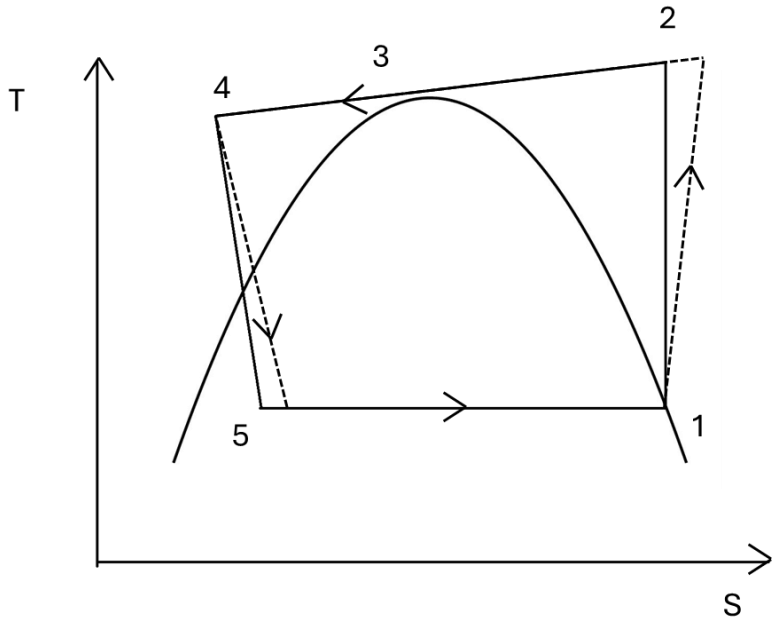

Figure 3.2: T-s diagram for a transcritical refrigeration system (TCRS).

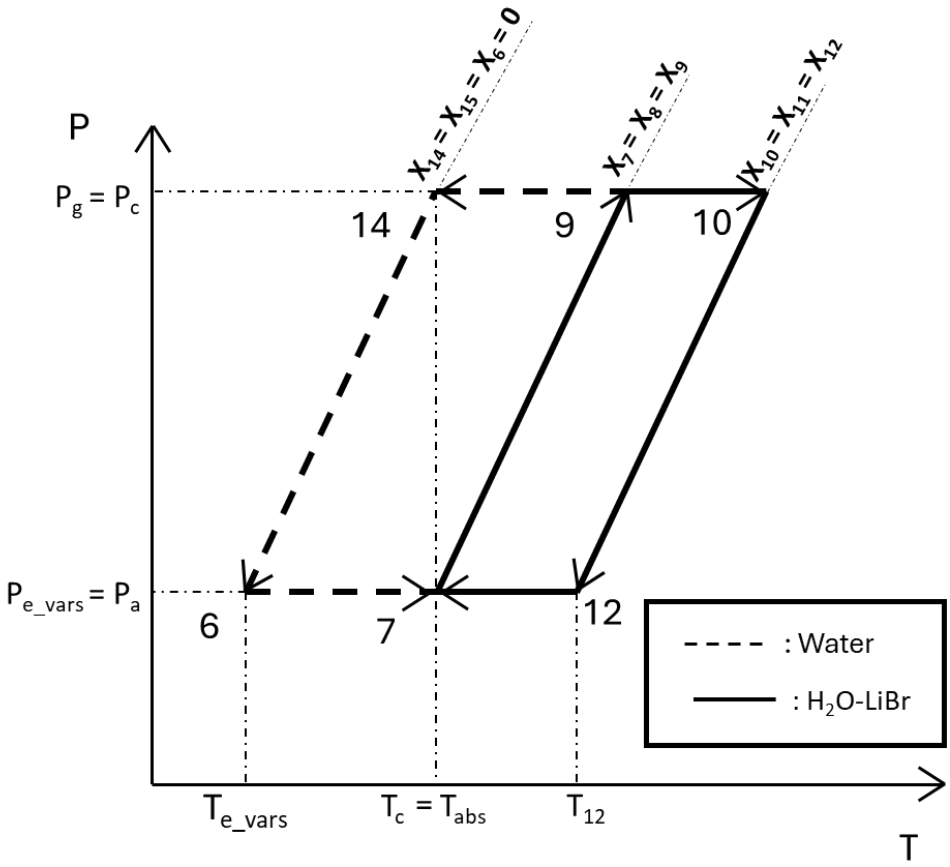

Figure 3.3: P-T-X diagram for single-effect VARS.

b. Series flow double effect VARS:

The system has a TCRS coupled with a series flow double effect VARS as shown in Figure 3.4. The refrigeration cycle mainly consists of two generators (LPG and HPG), condenser, evaporator, absorber, pump, two solution heat exchanger, and expansion valves. This system has three pressure levels: low pressure, medium and high. High pressure in HPG, low in evaporator and absorber, medium pressure in condenser and LPG. The solution is pumped to the heat exchangers from the absorber and then to the HPG, where the waste heat from gas cooler 1 of TCRS is delivered. The waste heat boil out the refrigerant from the solution. The vapour from HPG then comes into the LPG, thus heating the solution and being condensed. Vapour is produced at the outlet of LPG, which along with condensed water of the primary vapours flows into the condenser, the heat rejection also takes place during this process. The heat of condensation of primary vapour obtained from HPG is utilised in LPG to further obtain secondary vapour. This is followed by rejecting the heat to the surroundings. The refrigerant water leaves the condenser in the form of saturated liquid. The expansion valve reduces the pressure of stream where the cooling effect takes place. The P-T-X graph of the states are shown in Figure 3.5.

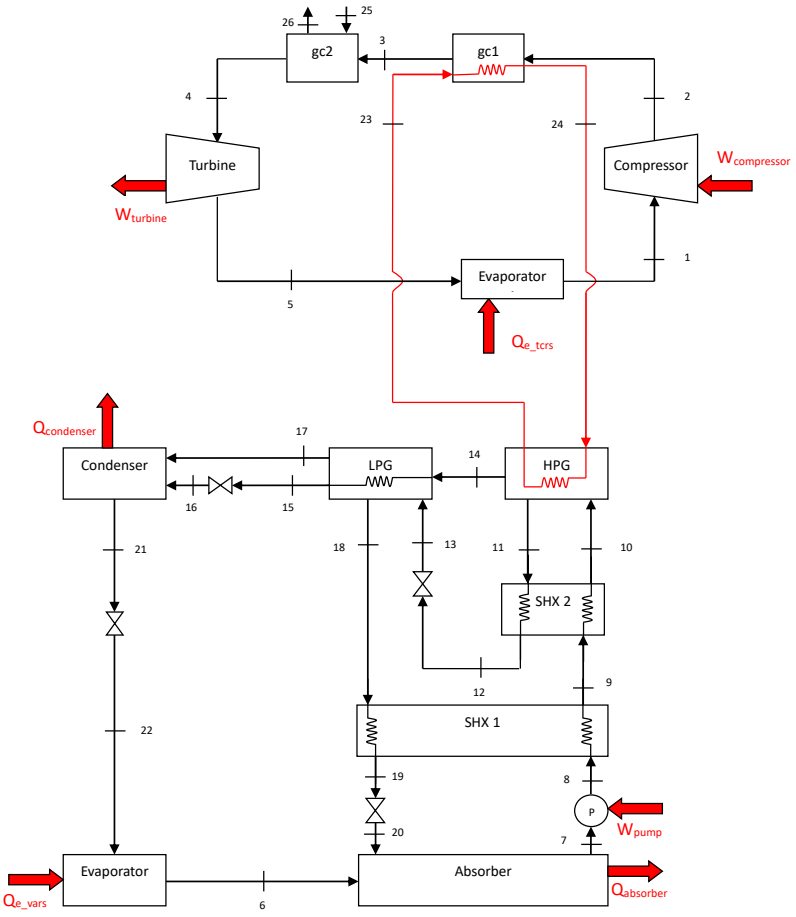

Figure 3.4: Schematic of TCRS integrated with a series flow double effect H2O-LiBr VARS

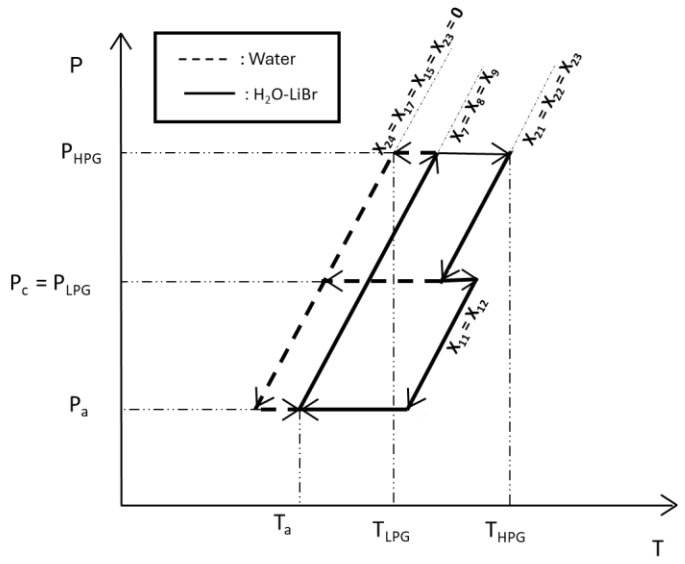

Figure 3.5: P-T-X diagram for series flow double-effect VARS.

c. Parallel flow double effect VARS:

The system has a TCRS combined with a parallel flow double effect VARS as shown in Figure 3.6. Like the series flow double effect VARS, the parallel flow also consists of two generators, i.e. HPG, and LPG, other than that it also contains two solution heat exchangers, absorber, evaporator, a number of expansion valves, condenser, and pump. In this, refrigerant water vapour is generated at different generator temperature and pressure in HPG and LPG at two stages. In this process, the solution travels from the absorber which is then pumped and distributed into the two parallel feet streams to the HPG and the LPG, respectively. Solution heat exchangers transfer the heat to cold stream from hot stream. Waste heat is taken from the TCRS and then transferred to HPG, where in refrigerant water vapour at a high-pressure and high temperature, departs from the solution. The water vapour is then condensed while passing through LPG and the latent heat of condensation from the refrigerant is utilised as a source of heat and which further generates extra refrigerant vapour from the second parallel feed solution, refrigerant water vapour produced in LPG is condensed within the condenser and the waste heat is dissipated to either an air-cooled type condenser or a water-cooled type condenser. The refrigerator is then used to feed the evaporator where the secondary cooling effect is delivered. The P-T-X graph of the states are shown in Figure 3.7.

The distribution ratio is symbolized by '*D*' which is defined as the fraction of total mass flow rate of solution leaving the absorber which is directed towards HPG.

$$D = \frac{\dot{m}_{HPG}}{\dot{m}_{solution,total}}$$

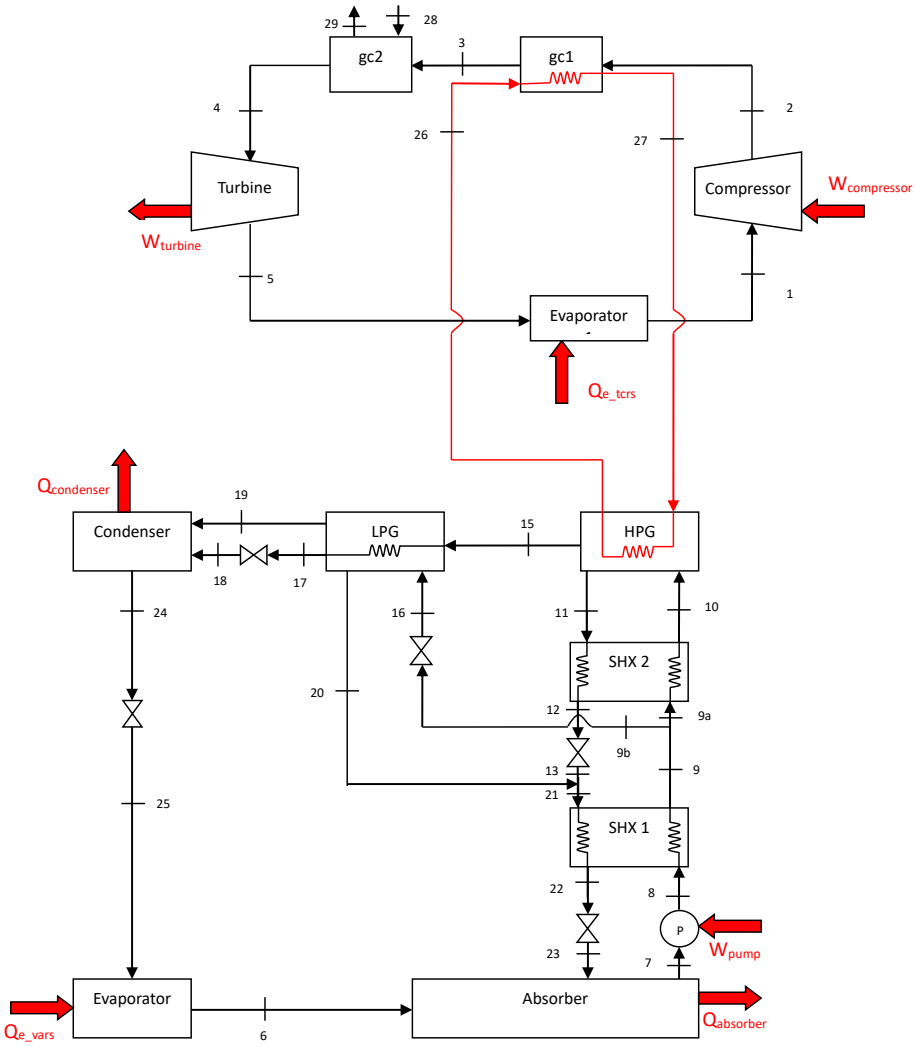

Figure 3.6: Schematic TCRS integrated with a parallel flow double effect H2O-LiBr VARS

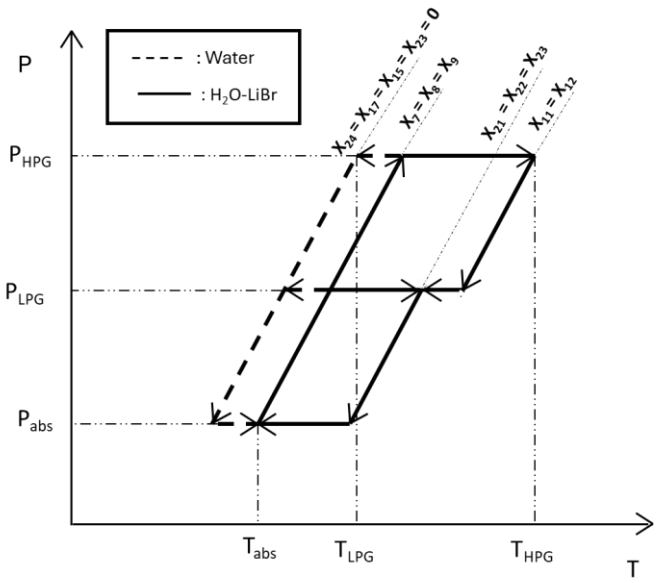

Figure 3.7: P-T-X diagram for parallel flow double-effect VARS.

3.2 Thermodynamic Analysis

To perform the Thermodynamic analysis we utilised mass conservation, first law of thermodynamics and second law of thermodynamics on all the components of the system.

a. Mass balance

$$\sum \dot{m}_i - \sum \dot{m}_o = 0 \quad (3.1)$$

b. Material balance

$$\sum (\dot{m}x)_i - \sum (\dot{m}x)_o = 0 \text{ (applicable to VARS only)} \quad (3.2)$$

ṁ is mass flow rate of H2O/LiBr solution and x is the concentration of H_2O/LiBr solution.

c. Energy balance

$$\left[\sum (\dot{m}h)_i - \sum (\dot{m}h)_o\right] + \left[\sum (\dot{Q})_i - \sum (\dot{Q})_o\right] + \dot{W} = 0 \quad (3.3)$$

The above equation is derived from the first law of thermodynamics which depicts the energy balance of the system.

The coefficient of performance is defined as the ratio of refrigerating capacity to the net power input.

COP of the TCRS is given by:

$$COP_{tcrs} = \frac{\dot{Q}_{e\_tcrs}}{\dot{W}_{tc}} \quad (3.4)$$

Where, $\dot{W}_{tc}=\dot{W}_c-\dot{W}_t$

The COP of the VARS is given by:

$$COP_{vars} = \frac{\dot{Q}_{e\_vars}}{\dot{Q}_{gen}+ \dot{W}_{pump}} \quad (3.5)$$

And the COP of the combined system is:

$$COP_{net} = \frac{\dot{Q}_{e\_tcrs}+ \dot{Q}_{e\_vars}}{\dot{W}_{tc}+ \dot{W}_{pump}} \quad (3.6)$$

d. Exergy analysis

Exergy is the maximum useful work that can be extracted from a system as it moves to thermodynamic equilibrium with its surroundings. It represents the system's ability to do work and accounts for both energy quantity and quality. Unlike energy, exergy is not conserved and is destroyed due to irreversibility such as friction, heat transfer, and mixing. It is widely used in efficiency analysis and optimization of thermodynamic systems.

The second law performance of a system is evaluated using exergetic efficiency. This efficiency metric reflects the fraction of input (fuel) exergy that is successfully converted into useful (product) exergy.

Here, the product refers to the intended outcome—in the case of a TCRS this is the cooling effect generated by the evaporator. The fuel, on the other hand, is the total net power input required to drive the system.

Thus, for a TCRS, the product exergy refers to the exergy of the cooling load extracted at the evaporator, while the fuel exergy corresponds to the net work supplied to operate the system.

Now, the exergetic efficiency of transcritical system is

$$\eta_{ex\_tcrs} = \frac{\dot{Q}_{e\_tcrs}\left|1-\frac{T_o}{T_{r\_tcrs}}\right|}{\dot{W}_{tc}} \tag{3.7}$$

where T_{r_tcrs} is the temperature of refrigerated space (in TCRS).

The exergetic efficiency of absorption system is

$$\eta_{ex\_vars} = \frac{\dot{Q}_{e\_vars}\left|1-\frac{T_o}{T_{r\_vars}}\right|}{m_{w1}(\varphi_{17}-\varphi_{16})} \tag{3.8}$$

where T_{r_vars} is the temperature of refrigerated space (in VARS) and $\varphi\ is\ exergy$.

Combining both we get, the net exergetic efficiency of the system as a whole, which is

$$\eta_{ex\_net} = \frac{\left(\dot{Q}_{e_{tcrs}}\left|1-\frac{T_o}{T_{r_{tcrs}}}\right|+\dot{Q}_{e_{vars}}\left|1-\frac{T_o}{T_{r_{vars}}}\right|\right)}{\dot{W}_{tc}+\dot{W}_{pump}} \tag{3.9}$$

3.3 Simulation

a. Assumptions

The system analysis is conducted based on the following assumptions:

- There is no pressure loss in any component due to any kind of irreversibility.
- In the VARS, the refrigerant exiting the evaporator and condenser is saturated vapor and saturated liquid, respectively.
- In the TCRS, The refrigerant exiting the evaporator is saturated vapour and the temperature at which CO_2 is leaving gas cooler 2 is assumed to be constant which is 40^0C

- The system is assumed to be designed for the space which has a temperature 5°C higher than the evaporator temperatures.

b. Parameters

1. Isentropic efficiency of turbine [16], $\eta_t = 0.6$
2. Isentropic efficiency of compressor [16],

   $\eta_c = 0.815 + 0.022r_p - 0.0041r_p^2 + 0.0001r_p^3$,

   where r_p is pressure ratio across compressor, $r_p = P_2/P_1$
3. Evaporator temperature in VARS, $T_{e\_vars} = 7°C$
4. Absorber and condenser temperatures, $T_a = T_{cond} = 35°C$.
5. Generator temperature, $T_g = 90°C$.
6. Temperature of HPG, $T_{HPG} = 130°C$
7. Temperature of LPG, $T_{LPG} = 80°C$
8. Effectiveness of solution heat exchanger, $\varepsilon_{shx} = 0.7$.
9. Effectiveness of gas cooler 1, $\varepsilon_{gc1} = 0.8$
10. Mass flow rate of refrigerant (CO_2) in the TCRS, $\dot{m} = 1kg/s$
11. Concentration of the mixture of two streams in combined TCRS and parallel flow VARS can be given by the formula given in [7],

$$\dot{x}_{21} = \frac{1}{\frac{D}{\dot{x}_{11}} + \frac{1-D}{\dot{x}_{20}}} \tag{3.10}$$

12. The distribution ratio,

$$D = \frac{\dot{m}_{HPG}}{\dot{m}_{solution,total}} \tag{3.11}$$

13. According to the temperature requirements T_{e_tcrs} can be varied over a range of -35^0C to -15^0C (the range is taken based on the applications of two evaporator used in ice-cream factories, and other cold storages). But the analysis shows that at the above conditions the system fails under -17.06^0C. So, the final operating range would be -35^0C to -17.06^0C.

CHAPTER 4: RESULTS AND DISCUSSION

4.1 Validation of combined TCRS and single-effect VARS

Figure 4.1 illustrates how the exergetic efficiency and COP of the TCRS vary with respect to the gas cooler pressure where evaporator temperature is –25°C and a gas cooler outlet temperature (T_4) of 40°C. As the gas cooler pressure increases, both the COP and exergetic efficiency initially rise, reaching their peak values at a certain pressure. Beyond this optimal point, both metrics begin to decline gradually. The optimal gas cooler pressure identified from the analysis is 9.846 MPa.

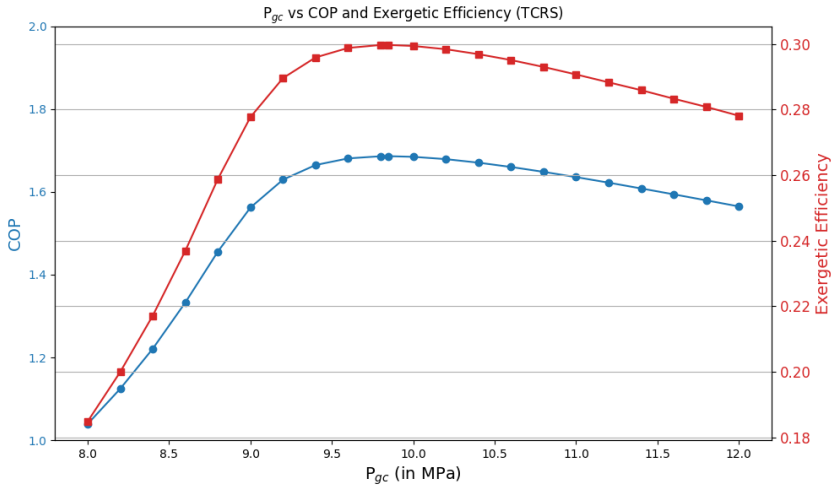

Figure 4.1: Diagram showing variation of exergetic efficiency and COP of TCRS with gas cooler pressure

In this Figure 4.2 we have plotted a graph between the exergetic efficiency and COP vs TCRS evaporator temperature (T_{e_tcrs}). In here a clear trend of COP of TCRS as well as combined system increasing.

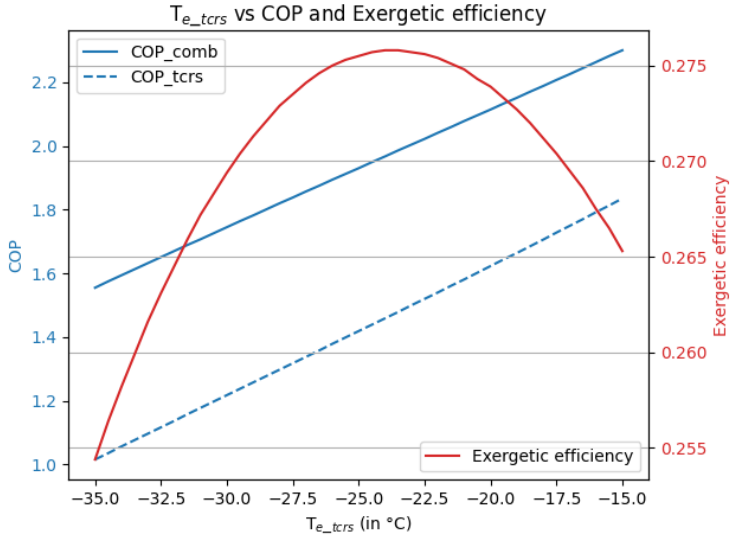

Figure 4.2: Diagram of COP (TCRS and combined) and Exergetic efficiency vs TCRS evaporator temperature (T_{e_tcrs}) of a combined TCRS and single-effect VARS.

From the exergy efficiency is given by equation 3.9. The first term in the numerator represents the exergy of the cooling effect. When the evaporator temperature increases, $\dot{Q}_{e\_tcrs}$ decreases slightly and the term,

$$\left|1 - \frac{T_o}{T_{r\_tcrs}}\right|$$

also decreases due to the T_{r_tcrs} approaching closer to T_0. The net work needed also decreases and up to a certain evaporator temperature the decrease in network is more than what is required to offset the decrease in the above terms. But after some temperature decrease in net work is not enough and exergetic efficiency decreases after that point leaving us with a maxima.

when evaporator temperature is –25°C in the TCRS and the gas cooler pressure is at optimum, the states, temperatures, specific enthalpies, specific entropies, mass flow rates, and concentrations of the H_2O/LiBr solution in each component for combined TCRS and single effect VARS are computed and presented in Table 4.1.

Table 4.1: System data derived from mass, material balance and first law of thermodynamics.

State	T (°C)	h (kJ/kg)	s (kJ/kg·K)	ṁ (kg/s)	x (% LiBr)
1	-25	-69.73	-0.7659	1	-
2	122.5	30.46	-0.7204	1	-
3	104.5	5.286	-0.7856	1	-
4	40	-191.54	-1.3750	1	-
5	-25	-209.19	-1.3278	1	-
6	7	2513	8.9730	0.0083	0
7	35	81.24	0.2188	0.0501	54.08
8	35	81.25	0.2188	0.0501	54.08
9	62.57	38.45	0.3963	0.0501	54.08
10	90	239.63	0.4748	0.0418	64.78
11	51.5	171.29	0.2758	0.0418	64.78
12	51.5	171.29	0.2758	0.0418	64.78
13	90	2669	8.663	0.0083	0
14	35	146.64	0.5051	0.0083	0
15	7	146.64	0.5248	0.0083	0

16	100	419.19	1.3071	0.0112	-
17	100	2676	7.3546	0.0112	-
18	25	104.9	0.3675	0.7392	-
19	88.6	371	1.1764	0.7392	-
20	25	104.9	0.368	1	-
21	30.71	128.64	0.4464	1	-
22	25	104.88	0.3672	1	-
23	29.99	125.68	0.4364	1	-

4.2 Combined TCRS and series flow double-effect VARS

Evaporator temperature is -25°C in the TCRS and 7°C in the VARS, with a turbine efficiency (η_t) of 0.6 and a gas cooler pressure (Pgc) of 13 MPa, the states, temperatures, specific enthalpies, specific entropies, mass flow rates, and concentrations of the H_2O/LiBr solution are provided in Table 4.2 and Table 4.3 for the combined TCRS and series-flow double-effect VARS, and the combined TCRS and parallel-flow double-effect (D = 0.2) VARS, respectively.

Table 4.2: System data derived from mass, material balance and first law of thermodynamics.

State	*T(°C)*	*h(kJ/kg)*	*s(kJ/kg.K)*	*ṁ(kg/s)*	*x(% LiBr)*
1	-25	-69.72	-0.7658	1	-
2	154.3	55.94	-0.7015	1	-
3	146.9	45.7	-0.7257	1	-
4	40	-215.2	-1.465	1	-
5	-25	-232	-1.42	1	-
6	7	2514	8.974	0.005453	-
7	35	81.17	0.2185	0.05298	54.08
8	35	81.17	0.2185	0.05298	54.08
9	61.09	135.2	0.387	0.05298	54.08
10	112.1	244.5	0.6894	0.05298	54.08
11	140	307.4	0.8021	0.05017	56.9

12	84.76	192	0.5041	0.05017	56.9
13	84.76	192	0.5041	0.05017	56.9
14	140	2758	7.673	0.002815	-
15	93.49	391.7	1.233	0.002815	-
16	35	391.7	1.3	0.002815	-
17	80	2650	8.611	0.002637	-
18	80	195.8	0.4509	0.04753	60.28
19	48.5	135.6	0.2721	0.04753	60.28
20	48.5	135.6	0.2721	0.04753	60.28
21	35	146.6	0.5051	0.005453	-
22	7	146.6	0.5247	0.005453	-
23	145	610.6	1.791	0.004807	-
24	145	2740	6.883	0.004807	-
25	30	125.8	0.4367	8.917	-
26	37	155.1	0.5321	8.917	-

Results obtained for the above system, is discussed in section 4.4.

4.3 Combined TCRS and parallel flow double-effect VARS

Table 4.3: System data derived from mass, material balance and first law of thermodynamics (D = 0.2).

State	T(°C)	h(kJ/kg)	s(kJ/kg.K)	ṁ(kg/s)	x(% LiBr)
1	-25	-69.72	-0.7658	1	-
2	154.3	55.94	-0.7015	1	-
3	146.9	45.7	-0.7257	1	-
4	40	-215.2	-1.465	1	-
5	-25	-232	-1.42	1	-
6	7	2514	8.974	0.006192	-
7	35	81.17	0.2185	0.06345	0.5408
8	35	81.17	0.2185	0.06345	0.5408

9	61.87	136.9	0.3919	0.06345	0.5408
9a	61.87	136.9	0.3919	0.006345	0.5408
9b	61.87	136.9	0.3919	0.05711	0.5408
10	83.04	181.8	0.5214	0.006345	0.5408
11	140	307.4	0.8021	0.002494	0.569
12	85.31	193.2	0.5072	0.002494	0.569
13	85.31	193.2	0.5072	0.002494	0.569
15	140	2758	7.673	0.003851	-
16	61.87	136.9	0.3919	0.05711	0.5408
17	93.49	391.7	1.233	0.003851	-
18	35	391.7	1.3	0.003851	-
19	80	2650	8.611	0.002341	-
20	80	195.8	0.4509	0.05477	0.6028
21	80.81	195.7	0.4534	0.05726	0.5992
22	48.74	134	0.2749	0.05726	0.5992
23	48.74	134	0.2749	0.05726	0.5992
24	35	146.6	0.5051	0.006192	-
25	7	146.6	0.5247	0.006192	-
26	145	610.6	1.791	0.004807	-
27	145	2740	6.883	0.004807	-
28	30	125.8	0.4367	8.917	-
29	37	155.1	0.5321	8.917	-

In Figure 4.3, plot of COP and Exergetic efficiency vs D(Distribution Ratio) is shown. Here we see a trend that both COP and Exergetic efficiency are decreasing as the Distribution Ratio(D) increases. We also notice that the rate at which COP and Exergetic efficiency are decreasing is lower at D=0.1 and starts increasing as the Distribution Ratio increases.

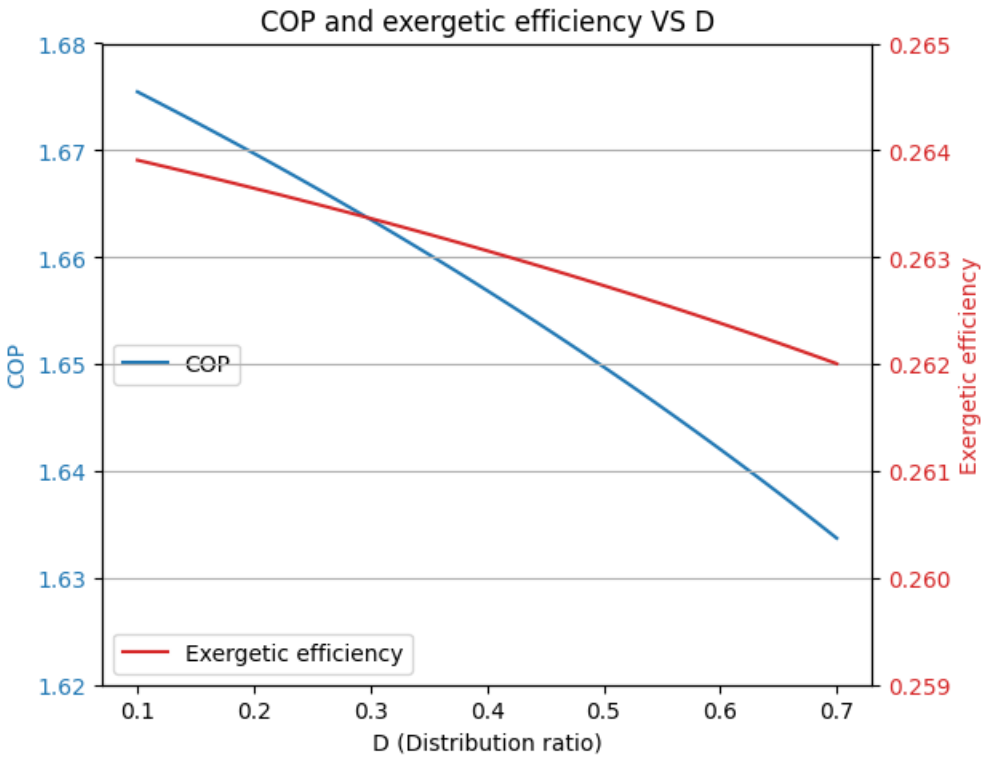

Figure 4.3: Diagram of COP and exergetic efficiency vs D (Distribution ratio) for combined TCRS and parallel flow double effect VARS.

This happens because increasing the solution distribution ratio causes more heat to be required in the HPG to desorb the refrigerant from the stronger solution. The HPG operates at a higher energy level, so any additional heat input here has lower thermodynamic efficiency compared to the LTG. Additionally, as more solution bypasses the LTG, its contribution to the overall desorption process reduces, even though it operates more efficiently. This imbalance leads to inefficient utilization of available heat sources, increasing the total heat input required from the TCRS without a proportional increase in cooling output, hence reducing COP.

Exergetic Efficiency decreases with an increase in Distribution ratio because more strong solution is directed to the high-temperature generator, which requires higher-grade heat input. This leads to greater irreversibility and exergy destruction due to inefficient use of high-quality energy. At the same time, the low-temperature generator, which operates more efficiently, becomes underutilized. Additionally, internal heat recovery processes become less effective, further increasing exergy losses. As a result, the system's ability to convert input energy into useful cooling decreases, lowering the overall exergy efficiency.

4.4 Comparison

The trend of COP with respect to the evaporator temperature of the TCRS for hybrid series-flow and hybrid parallel-flow systems, at different distribution ratios (D = 0.4, 0.5,

0.6), is presented in Figure 4.4. The COP increases as the evaporator temperature of the TCRS rises. With an increase in evaporator temperature, both the compressor work and the refrigeration effect decrease; however, the compressor work decreases more significantly than the refrigeration effect, which explains the observed trend. And it can also be seen that at a particular evaporator temperature, COP increases as the 'D' decreases and after a certain value it exceeds to that of the series-flow system. Also, after the point of convergence i.e. **-17.06 °C**, the heat supplied to the VARS is so low that the system is not at all contributing in refrigeration.

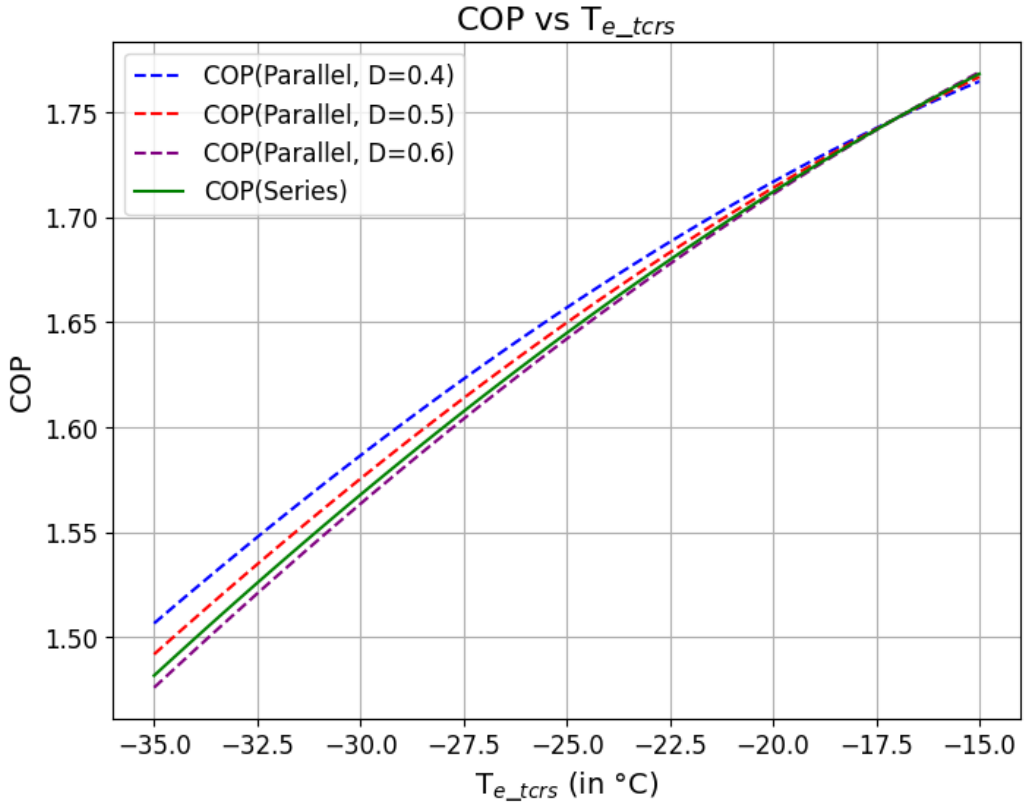

Figure 4.4: Diagram of COP vs T_{e_tcrs} for combined TCRS with series flow double effect VARS, and combined TCRS with parallel flow double effect VARS for distribution ratio 0.4, 0.5 and 0.6.

The Figure 4.5 shows the trend of exergetic efficiency with respect to the evaporator temperature of the TCRS for both hybrid series-flow and hybrid parallel-flow systems at different distribution ratios (D = 0.4, 0.5, 0.6). The exergetic efficiency is observed to initially increase and then decrease, exhibiting a maximum. The explanation for this behaviour is the same as that for the single-effect system. It can be observed that, at a constant evaporator temperature of the TCRS that the exergetic efficiency increases as the distribution ratio (D) decreases. Additionally, the exergetic efficiency of the hybrid series-flow system is lower than that of the hybrid parallel-flow system below a certain value of the distribution ratio.

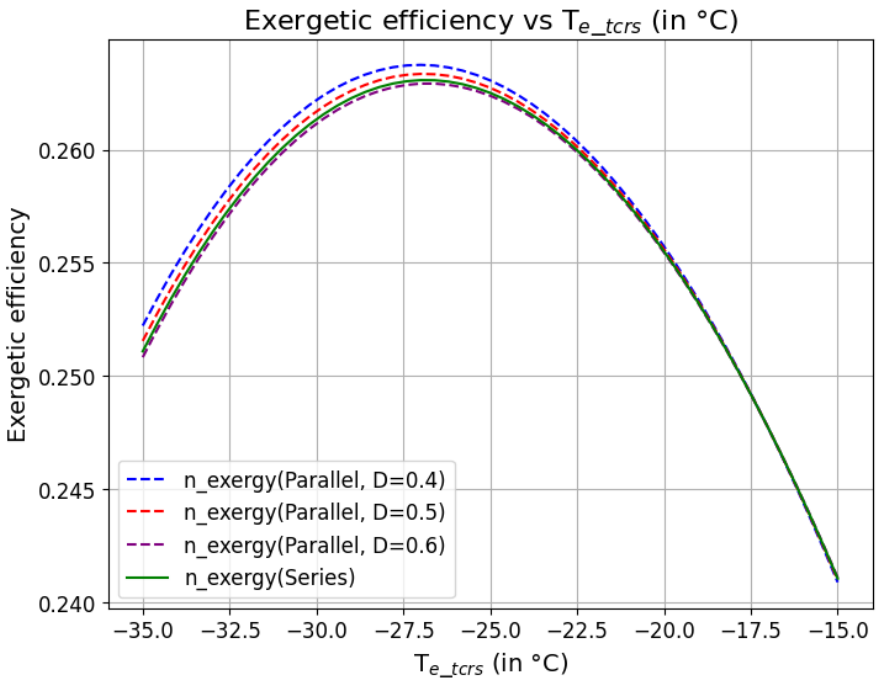

Figure 4.5: Diagram of exergetic efficiency vs T_{e_tcrs} for combined TCRS with series flow double effect VARS, and combined TCRS with parallel flow double effect VARS for distribution ratio 0.4, 0.5 and 0.6.

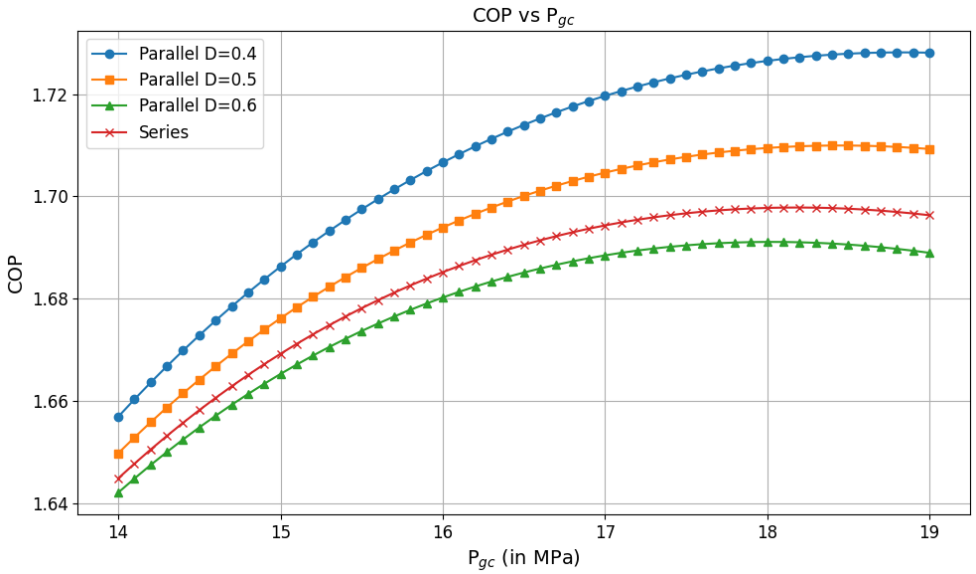

Figure 4.6: Diagram of COP vs P_{gc} for combined TCRS with series flow double effect vars, and combined TCRS with parallel flow double effect VARS for distribution ratio 0.4, 0.5 and 0.6.

In Figure 4.6, plot of COP and gas cooler pressure is shown. In here, we see a trend of that higher gas cooler pressure (P_{gc}) initially enhances the system's Coefficient of Performance (COP) by improving waste heat recovery and utilization. Higher P_{gc} elevates the temperature of the heat rejected by the TCRS, making it more suitable for driving the HPG in the VARS, thereby increasing refrigerant production efficiency. Additionally, the improved temperature matching between the TCRS and VARS components reduces thermodynamic losses. Also, at a given P_{gc}, COP is increasing with decreasing

distribution ratio and below a certain value of D parallel systems perform better compared to series.

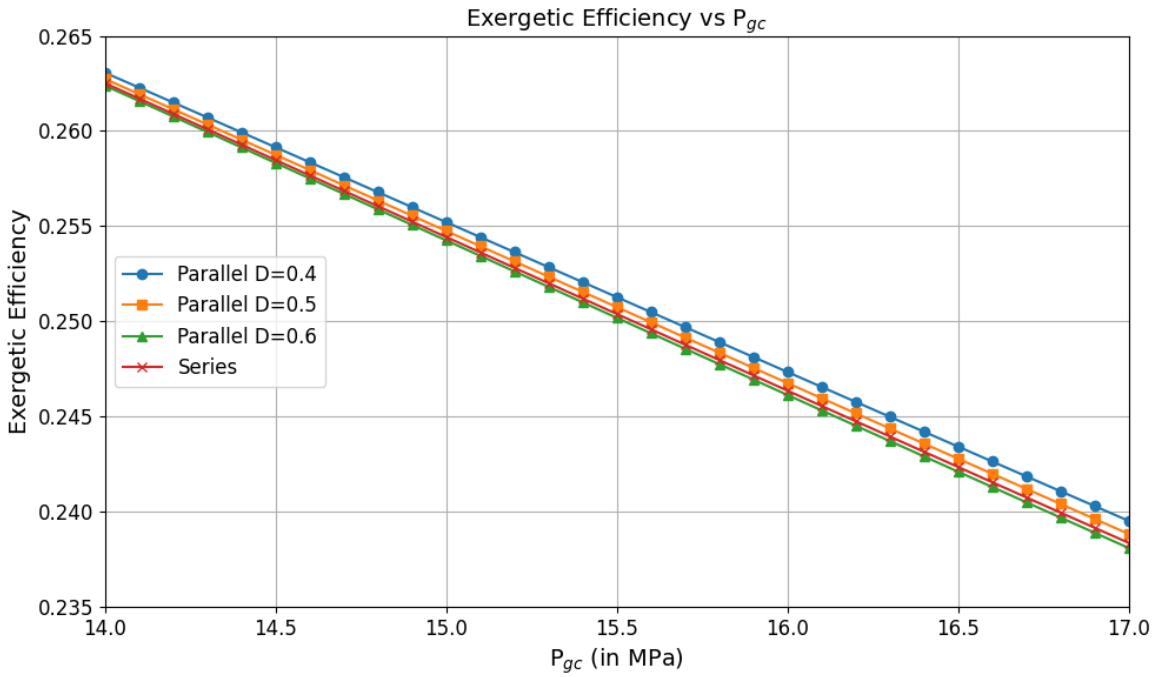

Figure 4.7: Diagram of Exergetic efficiency vs P_{gc} for combined TCRS with series flow double effect VARS, and combined TCRS with parallel flow double effect VARS for distribution ratio 0.4, 0.5 and 0.6.

In Figure 4.7, plot of exergetic efficiency vs P_{gc} is shown. In here, we see a trend of exegetic efficiency decreasing as we increase P_{gc}. This can be attributed to the fact that as we increase the P_{gc}, more heat is supplied to VARS and it would produce more refrigeration effect and TCRS system will produce less. The evaporator temperature of TCRS is lower than that of VARS and in the exergy efficiency formula (equation 3.9). Refrigeration effect of TCRS is multiplied by a larger term compared to VARS and the net work done in the denominator also decreases contributing to the trend of decreasing exergetic efficiency. We also see that as we increase solution distribution ratio(D), the exergetic efficiency decreases and at a certain point becomes less than in series configuration.

Figure 4.8 shows how the ratio of the cooling effects of VARS and TCRS(Q_{e_vars}/Q_{e_tcrs}) changes as the evaporator temperature of TCRS increases. The graph shows a downward trend. This happens because when the evaporator temperature goes up, the cooling effect of TCRS (Q_{e_tcrs}) gets smaller. At the same time, the heat released in gas cooler 1 also drops. Thus, less amount of heat is supplied to the generator of the VARS system, which means the cooling effect of VARS (Q_{e_vars}) also drops—but it drops faster than Q_{e_tcrs}.

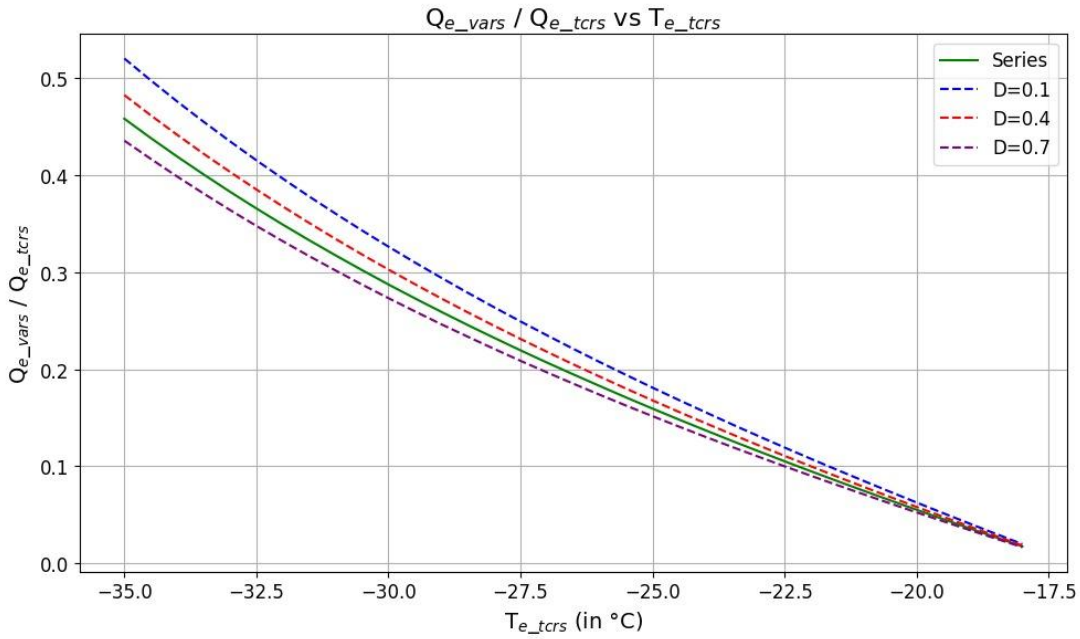

Figure 4.8: Diagram representing supplementary refrigeration effect derived from different configurations of VARS expressed as a ratio to the refrigeration effect from TCRS at optimal conditions of TCRS.

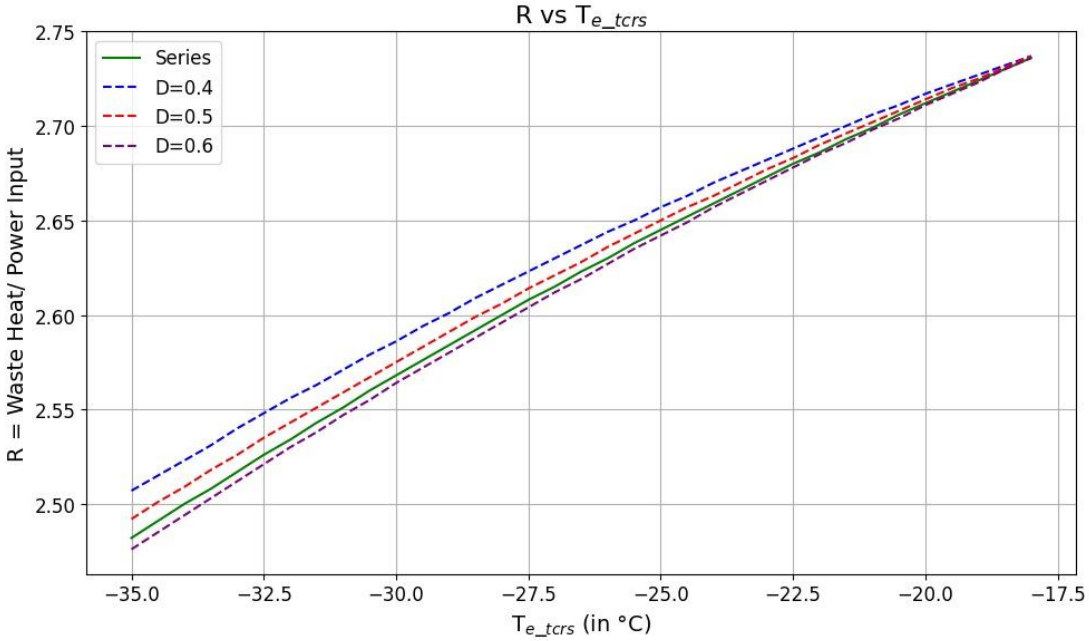

Figure 4.9: Heat rejected in comparison to net work input to TCRS for a variation of evaporator temperature of TCRS for different configurations.

Figure 4.9 represents how the ratio of waste heat to power input (R) changes with the evaporator temperature (Te_tcrs). As Te_tcrs increases, R also goes up. This happens because the input work gets lower when Te_tcrs rises, while the amount of waste heat that needs to be removed in gas cooler 2 stays the same. So, the increase in R makes sense.

CHAPTER 5: CONCLUSIONS AND FUTURE OUTLOOK

5.1 Conclusions

The main conclusions from this study are:

- At a gas cooler pressure of 14 MPa and distribution ratio (D) below 0.57, the hybrid parallel flow VARS system outperforms the hybrid series flow VARS system in both COP and exergetic efficiency.
- Under specific conditions (T_{e_tcrs} = -25°C, P_{gc} = 14 MPa, D = 0.1), the COP values are 1.42 for TCRS, 1.64 for hybrid series flow VARS, and 1.68 for hybrid parallel flow VARS — reflecting an 18.06% increase over TCRS and a 1.86% improvement over the series configuration.
- Similarly, under same conditions the exergetic efficiencies recorded are 25.22% (TCRS), 26.25% (series VARS), and 26.39% (parallel VARS), marking a 4.66% enhancement over TCRS and a marginal 0.53% advantage over the series flow system.

5.2 Future Outlook

There is considerable potential for developing and exploring additional impactful configurations of VARS systems. Moreover, notable differences may arise between theoretical or analytical predictions and actual experimental results, highlighting the need for further investigation and validation.

REFERENCES

1. Ge, Y. T., and S. A. Tassou. 2011. "Thermodynamic Analysis of Transcritical CO2 Booster Refrigeration Systems in Supermarket." *Energy Conversion and Management* 52: 1868–1875. https://doi.org/10.1016/j.enconman.2010.11.015.
2. Haq, Md. Zahurul, Md. Shaumik Rahman Ayon, Md. Waheduzzaman Bosunia Nouman, and Raghav Bihani. 2022. "Thermodynamic Analysis and Optimisation of a Novel Transcritical CO2 Cycle." *Energy Conversion and Management* 273: 116407. https://doi.org/10.1016/j.enconman.2022.1164073.
3. Joybari, Mahmood Mastani, and Fariborz Haghighat. 2016. "Exergy Analysis of Single Effect Absorption Refrigeration Systems: The Heat Exchange Aspect." *Energy Conversion and Management* 126: 799–810. https://doi.org/10.1016/j.enconman.2016.08.029.
4. Soliman, Ahmed Saad, Shuping Zhu, Li Xu, Junguo Dong, and Ping Cheng. 2021. "Design of an H2O-LiBr Absorption System Using PCMs and Powered by Automotive Exhaust Gas." *Applied Thermal Engineering* 191: 116881. https://doi.org/10.1016/j.applthermaleng.2021.116881.
5. Arshi Banu, P.S., and N.M. Sudharsan. 2018. "Review of Water Based Vapour Absorption Cooling Systems Using Thermodynamic Analysis." *Renewable and Sustainable Energy Reviews* 82: 3750–3761. https://doi.org/10.1016/j.rser.2017.10.092
6. Xie, G. 2023. "Thermodynamic Analysis and Multi-Objective Optimization of a Waste Heat Driven S–CO2 Recompression Brayton Cycle–Transcritical CO2 Cooling Cycle for Shipboard Application." *Energy* 265: 126332. https://doi.org/10.1016/j.energy.2022.126332.
7. Siddique, Sefat Mahmud, M. Muhtasim Uzzaman, M. Monjurul Ehsan, and Yasin Khan. 2025. "Thermal Analysis of a Novel Configuration of Double Effect Absorption System Cascaded with Ejector and Injection Enhanced Compression Refrigeration Cycle." *Energy Conversion and Management* 326: 119435. https://doi.org/10.1016/j.enconman.2023.119435.
8. Ma, W. B., and S. M. Deng. 1996. "Theoretical Analysis of Low-Temperature Hot Source Driven Two-Stage LiBr/H2O Absorption Refrigeration System." *International Journal of Refrigeration* 19 (2): 141–146.
9. Xu, G. P., Y. Q. Dai, K. W. Tou, and C. P. Tso. 1996. "Theoretical Analysis and Optimization of a Double-Effect Series-Flow-Type Absorption Chiller." *Applied Thermal Engineering* 16 (12): 975–987. https://doi.org/10.1016/S1359-4311(96)00011-7.
10. Xu, G. P., and Y. Q. Dai. 1997. "Theoretical Analysis and Optimization of a Double-Effect Parallel-Flow-Type Absorption Chiller." *Applied Thermal Engineering* 17 (2): 157–170. https://doi.org/10.1016/S1359-4311(96)00021-X.

11. Cimsit, Canan. 2018. "Thermodynamic Performance Analysis of the Double Effect Absorption-Vapour Compression Cascade Refrigeration Cycle." *Journal of Thermal Science and Technology*, Paper No. 17-00593.

12. Gomri, Rabah. 2009. "Second Law Comparison of Single Effect and Double Effect Vapour Absorption Refrigeration Systems." *Energy Conversion and Management* 50: 1279–1287. https://doi.org/10.1016/j.enconman.2009.01.019.

13. Gomri, Rabah. 2010. "Investigation of the Potential of Application of Single Effect and Multiple Effect Absorption Cooling Systems." *Energy Conversion and Management* 51 (7): 1629–1636. https://doi.org/10.1016/j.enconman.2009.12.039.

14. Kaita, Y. 2002. "Simulation Results of Triple-Effect Absorption Cycles." *International Journal of Refrigeration* 25 (8): 999–1007. https://doi.org/10.1016/S0140-7007(01)00100-1.

15. Arora, Akhilesh, Nikhil Kumar Singh, Saksham Monga, and Omesh Kumar. 2011. "Energy and Exergy Analysis of a Combined Transcritical CO2 Compression Refrigeration and Single Effect H2O-LiBr Vapour Absorption System." *International Journal of Exergy* 9 (4): 453–471.

16. Robinson, D.M. and Groll, E.A. (1998) 'Efficiencies of transcritical CO2 cycles with and without an expansion turbine', International Journal of Refrigeration, Vol. 21, No. 7, pp.577–589.

17. Dubey, A.M., Kumar, S., and Agrawal, G.D. 2014. "Thermodynamic Analysis of a Transcritical CO_2/Propylene (R744–R1270) Cascade System for Cooling and Heating Applications." Energy Conversion and Management 86: 774–783. https://doi.org/10.1016/j.enconman.2014.05.105.

18. Vaccaro, G., Milazzo, A., and Talluri, L. 2023. "Thermodynamic Assessment of Trans-Critical Refrigeration Systems Utilizing CO_2-Based Mixtures." International Journal of Refrigeration 147: 61–70. https://doi.org/10.1016/j.ijrefrig.2022.09.013.

19. Yang, P., Yuan, M., Liu, Z., Xie, N., Liu, Y., Yang, S. 2021. Multi-objective optimization and life cycle assessment of a cascade system integrating LiBr/H_2O absorption refrigeration with transcritical CO_2 power cycle. Energy Conversion and Management 244: 114453. https://doi.org/10.1016/j.enconman.2021.114453.

20. Pátek, Jaroslav, and Jaroslav Klomfar. 2006. "A Computationally Effective Formulation of the Thermodynamic Properties of LiBr–H_2O Solutions from 273 to 500 K over Full Composition Range." International Journal of Refrigeration 29 (5): 566–578. https://doi.org/10.1016/j.ijrefrig.2005.10.007.

BRIEF BIO-DATA OF THE AUTHORS

Karanjit Singh

Mr. Karanjit Singh joined the Department of Mechanical and Industrial Engineering at IIT Roorkee in 2021 to pursue a bachelor's degree in mechanical engineering. He has a strong interest in HVAC engineering and is also actively involved in the field of machine learning. He hopes to apply his knowledge in both areas to solve real-world engineering problems.

Nikita

Ms. Nikita joined the Department of Mechanical and Industrial Engineering at IIT Roorkee in 2021 to pursue a bachelor's degree in mechanical engineering. She is passionate about thermodynamic and structural analysis. She has also been actively involved in animal welfare during her stay on campus.

Varnit Gupta

Mr. Varnit Gupta joined the Department of Mechanical and Industrial Engineering at IIT Roorkee in 2021 to pursue a bachelor's degree in mechanical engineering. He has interests in powerplant engineering and solid mechanics. He is also exploring stock market and is passionate about finance.